Applied Acoustics xxx (2008) xxx–xxx

Contents lists available at ScienceDirect

Applied Acoustics

journal homepage: www.elsevier.com/locate/apacoust

Textural analyses of multibeam sonar imagery from Stanton Banks, Northern Ireland continental shelf

Ph. Blondel *, O. Gómez Sichi

Department of Physics, University of Bath, Claverton Down, Bath BA2 7AY, UK

ARTICLE INFO

Available online xxxx

PACS:
43.60.Lq
91.50.Ey
91.50.Bd

Keywords:
Multibeam imagery
Seafloor classification
Acoustic textures

ABSTRACT

The mapping of marine habitats mainly relies on acoustic techniques and there is a clear need for reliable classification methods supplementing the interpreter with as much quantitative information as possible. This article presents textural analyses of multibeam sonar imagery from Stanton Banks, on the continental shelf off Northern Ireland. TexAn, originally developed for the textural analysis of sidescan sonar imagery, was tested over an area of ~72 km^2 surveyed in 2005 by the European MESH project. The multibeam imagery is affected by several artefacts, including strong uncorrected angular variations in some tracks, and the acquisition of some tracks with very different aspects. The results from unsupervised classification of the imagery, using K-Means, match well the interpretations that can be made using concurrent bathymetric data and visual observations acquired in a later cruise. Textural analyses successfully detect faint trawlmarks and distinguish between the different types of seafloor, including variations within sediments, rocky outcrops and gullied terrains.

1. Rationale

Large-scale acoustic mapping of marine habitats began in earnest about a decade ago, with the collaborative research efforts of North American institutions to create national marine sanctuaries like Stellwagen Bank (e.g. [1]). It has now become a full-blown field of study, with many successful applications throughout the world (e.g. [2–5]). Habitat mapping aims at integrating biological and geological studies with sonar imaging of the seabed and overlying features. Although each mapping system has its own advantages and limitations (e.g. coverage vs. resolution), multibeam sounders have proved the most versatile and complete instrument, providing background topography and showing seabed features in relatively high detail (e.g. [6]). For most modern surveys, repeatability and time evolution have become key factors (e.g. [7]). Owing to the amount of data collected in a typical survey, and the subtle variations in acoustic responses of some seabed features, visual interpretation of sonar records is no longer an option. Acoustic classification systems must provide quantitative data in a reasonable time, and supplement the interpreter with as much information as possible.

There are many approaches to acoustic seabed classification, and end-users from different fields aim for different objectives. To conciliate the different aims, a workshop was organised in 2006 to bring together both providers of acoustic classification systems and users of sonar imagery and (potentially) classified maps [8]. This workshop was held at the University of Ulster, Coleraine, Northern Ireland, within the framework of the Interreg IIIB project MESH ("*Mapping European Seabed Habitats*") [9]. A common dataset of multibeam bathymetry and imagery was issued to all participants before the meeting, for treatment with different approaches. These included reprocessing of the raw acoustic measurements as well as processing with acoustic classification systems, and the results are presented in companion papers in this issue. The present article focuses on the analysis of the multibeam imagery with *TexAn*, a proprietary software from the University of Bath originally designed for textural analyses of sidescan sonar imagery [10,11]. Section 2 describes the general method used to analyse acoustic textures of sonar images with TexAn. Section 3 shows its application to the multibeam imagery from the common MESH dataset. Section 4 discusses the results, comparing them with those from other studies and with available ground-truth. It also makes recommendations for improving the processing of the input multibeam imagery. Finally, Section 5 provides a synthesis and guidelines for further uses of the textural analyses of multibeam imagery.

2. Method

2.1. Acoustic textures – TexAn software

Images, whatever their origin, are intuitively mapped on the basis of their tonal and textural properties. In the case of sonar

* Corresponding author. Tel.: +44 01225 385237; fax: +44 01225 386110.
E-mail address: pyspb@bath.ac.uk (Ph. Blondel).

0003-682X/$ - see front matter © 2008 Elsevier Ltd. All rights reserved.
doi:10.1016/j.apacoust.2008.07.015

images, whether acquired with a sidescan or a multibeam, tonal information is directly related to the amount of acoustic energy backscattered, generally represented as grey levels. Different statistical indices (e.g. extrema and median values) can be used to quantify local information. These first-order statistics quantify the distribution of the grey levels, but do not take into account their positions relative to each other (i.e. the acoustic textures). These textures, however, account for most of the information in acoustic images, as countless studies have shown (e.g. [7,10–21]). The local textural properties can be summarised as rough or smooth, varied or homogeneous, repetitive or random, and hence can help in distinguishing between different areas and features in the images. Quantitative textural measurements (second-order statistics) can be extracted from the image with various techniques, the most efficient being stochastic [12]. This original theoretical work was supplemented with practical applications to sonar imagery by [10,13–16] and others, showing that Grey-Level Co-occurrence Matrices (GLCMs) are optimally adapted. GLCMs address the average spatial relationships between pixels of a small region. Experiments on human vision (Julesz, 1973, *in* [10]) demonstrated that the eye could not distinguish between textures with different second-order statistics, proving GLCMs could be used to go further than traditional, visual interpretation alone.

The University of Bath software *TexAn* uses the indices derived from GLCMs calculated for each pixel in the images and clusters relevant textural indices into appropriate groups, related to specific acoustic processes and structures on/in the seabed. This software has been validated on sidescan sonar imagery in a variety of environments (e.g. [10,11,15,17,18]), and recent developments [19,20] showed its promise with multibeam sonar imagery.

To quantify the textures, *TexAn* calculates GLCMs $\{P_D(i,j)\}$ over the entire image, within moving windows of a set size. Each element $P_D(i,j)$ expresses the relative frequency of occurrence, within the window, of two pixels with the respective grey levels i and j at $D(SZ,\theta)$ (Euclidian distance SZ and angle θ) from one another. If the image is quantified with NG grey levels, the GLCMs will be NG $\times$ NG arrays. The distance $D(SZ,\theta)$ is very sensitive to the orientation θ. This is particularly true for sonar images, in which the insonification angle can vary both along and across track. In order to avoid changes in the textural indices of a feature with non-isotropic texture, insonified at different angles, the GLCMs are calculated for the angles $\theta = 0°$, 45°, 90° and 135° and then averaged, following Refs. [13] and [10]. Hence the only remaining computational parameters are the inter-pixel displacement SZ, the number of grey levels (NG) and the size of the computational window (WS). The matrices resulting from the calculations described above, however, cannot be interpreted directly in an easy way (as can be seen from the examples in Fig. 1). Therefore, their information is summarised in a set of statistical measures, called 'indices'. More than 25 different textural indices have been described in the literature (e.g. [10,13]), but a detailed evaluation of their performance has shown that the combination of two indices (entropy and homogeneity) seems sufficient to explain nearly all the textural variability in sidescan sonar images [10,14]. The entropy index measures the lack of spatial organisation within the computational window, and hence is a measure of the local amount of 'chaos'. It will be higher for rough textures, and lower for organised heterogeneities such as ripples. Textural homogeneity is a measure of the amount of local similarities within the window. The index is similar to the 'inverse-difference moment' of [15] and will increase in windows with less contrast (fewer grey levels). An additional factor was introduced by [10] in the calculation of this index to ensure invariance during linear grey-level transformations (such as those caused by variations in TVG or AVG from one computation window to another). Fig. 1 shows how GLCMs can vary for even simple textures, and how entropy and homogeneity can clearly distinguish between even complex textures. The textural indices having been chosen, there is now a need to identify the best combination(s) of inter-pixel displacement SZ, number of grey levels NG and computation window size (WS) that maximise the difference between regions in the entropy/homogeneity space (also called feature space).

2.2. Optimisation of textural parameters

This optimisation is performed by choosing Training Zones representative of the acoustic facies encountered in the entire image and which one wants to distinguish. These Training Zones need to be square (to avoid over-emphasis on one direction in the image). They need to be large enough to be statistically significant for a large range of window sizes, WS, as their size influences the number of times independent values can be measured. For example, for a Training Zone of 100 $\times$ 100 pixels, choosing $WS = 90$ pixels can only yield 100 independent measurements of entropy and homogeneity, whereas choosing $WS = 10$ pixels can yield 8100 independent measurements. Conversely, Training Zones need to be small enough to encompass only one type of acoustic texture.

The first parameter to vary is the size WS of the computation window. It can in theory take any value smaller than the size of the Training Zones, but is in fact constrained by its physical significance. Smaller values (10 pixels or smaller) will increase the contributions of very close pixels and measure the high-frequency backscatter variations in the image (generally attributable to speckle, particularly in multibeam imagery). Larger values (close to the size of the Training Zones) will instead look at lower-frequency variations in the image, and will have a higher probability of mixing two texturally distinct regions or missing intrinsic textural characteristics. Finally, the difference in insonification angles from one edge of the computation window to the opposite edge will need to be taken into account, although it will be smaller for multibeam systems than for sidescan sonars.

The second textural parameter is the displacement size SZ within the window. It is intricately linked to its size WS. Values close to WS will emphasize variations of the same size as the computation window, whereas the smaller values will emphasize the noise within the window. Again, the influence of the variations in ensonification angle between pixels separated by SZ should be accounted for. If small-scale variations in large structures are to be detected, a small SZ should be associated to a large WS. However, if the structures to be observed are characterised by variations of a wavelength comparable to their dimensions, SZ should be slightly less than the size of the window. Based on practice with both sidescan and multibeam imagery, the optimal values of SZ usually lie close to $WS/2$.

Last but not least, the number of grey levels NG will affect both the speed of the computation and its accuracy. As NG decreases, there are less and less variations around the mean grey levels (smoothing of the dynamic range). For high values (as close to the full dynamic range as possible), the textures are more likely to appear rougher and more heterogeneous. Systematic tests show that, as NG decreases from 256 (8-bit dynamics) to 16 (4-bit dynamics), entropy will decrease linearly by 50% at most, and homogeneity by 30%. The overall computation time varies approximately as $o(NG^2)$. For 8-bit dynamic ranges, practice shows that optimal numbers are usually between 32 and 128, depending on the quality of the processing and the amount of noise in the image.

The combination(s) of optimal values are found by systematically varying NG, WS and SZ and calculating entropy and homogeneity at each point in the Training Zones. The separation between Training Zones is visualised in the feature space. It can be tested quantitatively, but it is very sensitive to the overlap of poorly defined (or complex) classes and a contextual assessment of the separation is preferred. For example, dunes will be seen either as "dunes" for large values of WS or as alternate "strips" for small

Please cite this article in press as: Blondel Ph, Gómez Sichi O, Textural analyses of multibeam sonar imagery from Stanton Banks, ..., Appl Acoust (2008), doi:10.1016/j.apacoust.2008.07.015

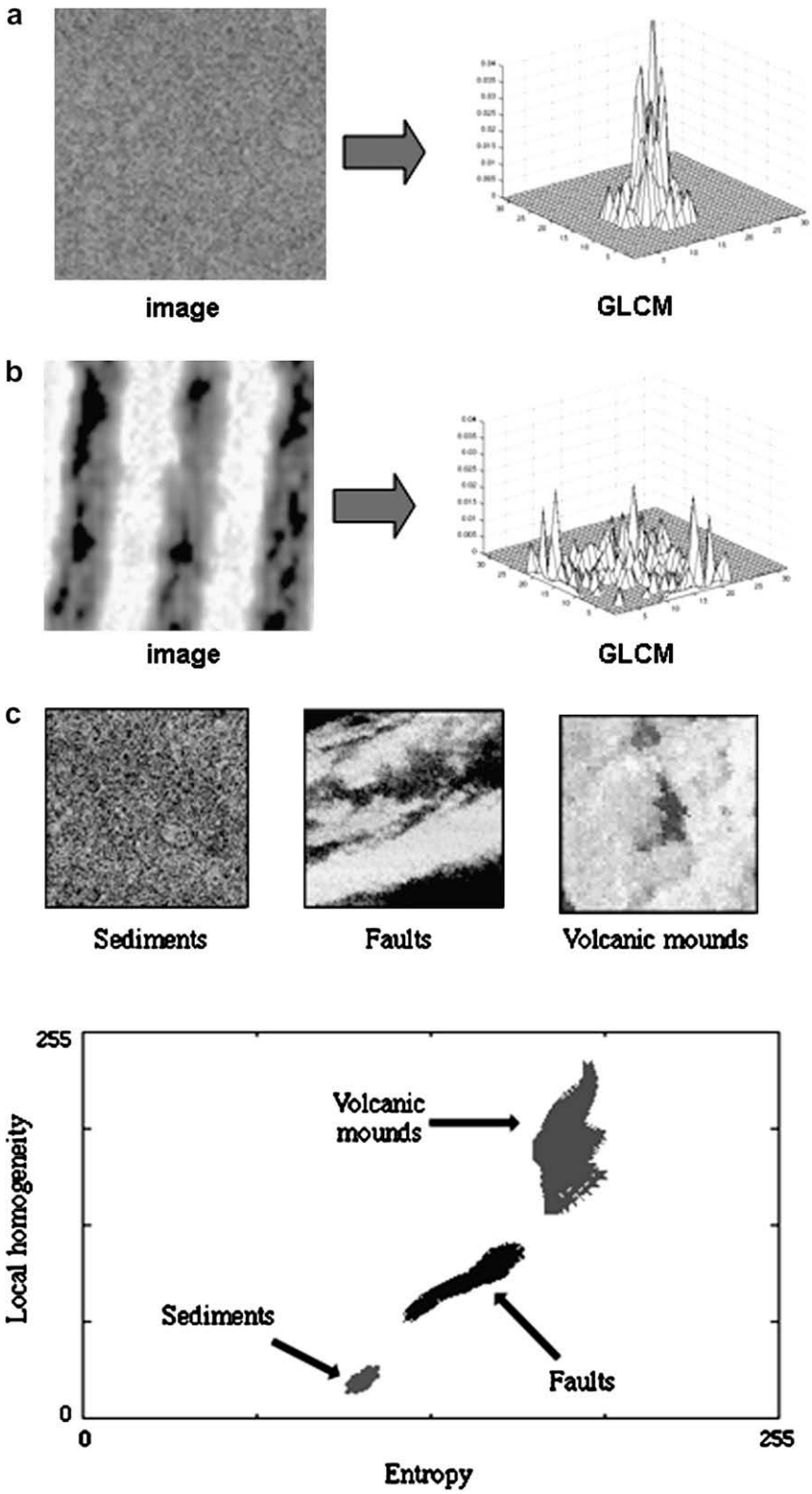

Fig. 1. (a) Sonar image of a smooth texture (mud) with very few grey levels and its resulting GLCM, with one peak showing the most common grey level (the width of the peak is proportional to the variations around this most common level); (b) Image of a regular texture (sonar image of sand ripples) with two main grey levels and resulting GLCM; the main peaks are related to the two levels, their occurrences close to each other and their relative distributions. As can be seen, even for very simple textures, GLCMs cannot be interpreted easily on their own. (c) Three images of distinct terrains can be distinguished from the entropy and homogeneity of the GLCMs (see text for details).

values of *WS*. Similarly, poorly contrasted rocks might be seen as "smooth sediments" for too low values of *NG*. The optimal separation between classes has therefore to be balanced with the choice of textural computation parameters. Systematic tests are carried for $NG = 2^n$ (with n varying from 3, i.e. 8 possible grey levels, all the way to the full dynamic range available), *WS* varying from 10 to 80 pixels by steps of 10 pixels, and *SZ* ranged from 10 to ($WS - 10$) by steps of 5 pixels. In the entropy/homogeneity feature

Please cite this article in press as: Blondel Ph, Gómez Sichi O, Textural analyses of multibeam sonar imagery from Stanton Banks, ..., Appl Acoust (2008), doi:10.1016/j.apacoust.2008.07.015

space, it is important that the different clouds of points be well separated, but that there still is enough variation to identify differences within each facies/potential habitat type.

2.3. Classification of textural indices

The optimisation of the textural computation parameters produces (generally) one or (sometimes) several combinations of (*NG*, *WS*, *SZ*) values for which the Training Zones can be well separated from their entropy and homogeneity values alone. The next step of *TexAn* is then to extend these calculations to the entire image, calculating entropy and homogeneity for each point in the dataset and classifying them into different regions or clusters, which then have to be identified and associated to image facies and processes on/in the seabed. Different algorithms have been used, ranging from feature-space guided clustering [10,17] to classification using Look-Up Tables for specific objects (e.g. mines in [11]) and unsupervised classification algorithms like ISODATA [7]. Because of the higher control it allows on the different processing parameters, more recent applications have tended to use the K-Means algorithm.

K-means clustering is a rapid and simple method to partition a feature space [21]. Here, it aims at dividing the individual measurements of entropy and homogeneity into several mutually exclusive clusters. It works iteratively by minimising the mean of the distance between each sample and the nearest cluster centre, moving measurements between clusters until convergence. The points in the clusters will be as close as possible, whilst the distance between clusters will be as large as possible. Several metrics can be used

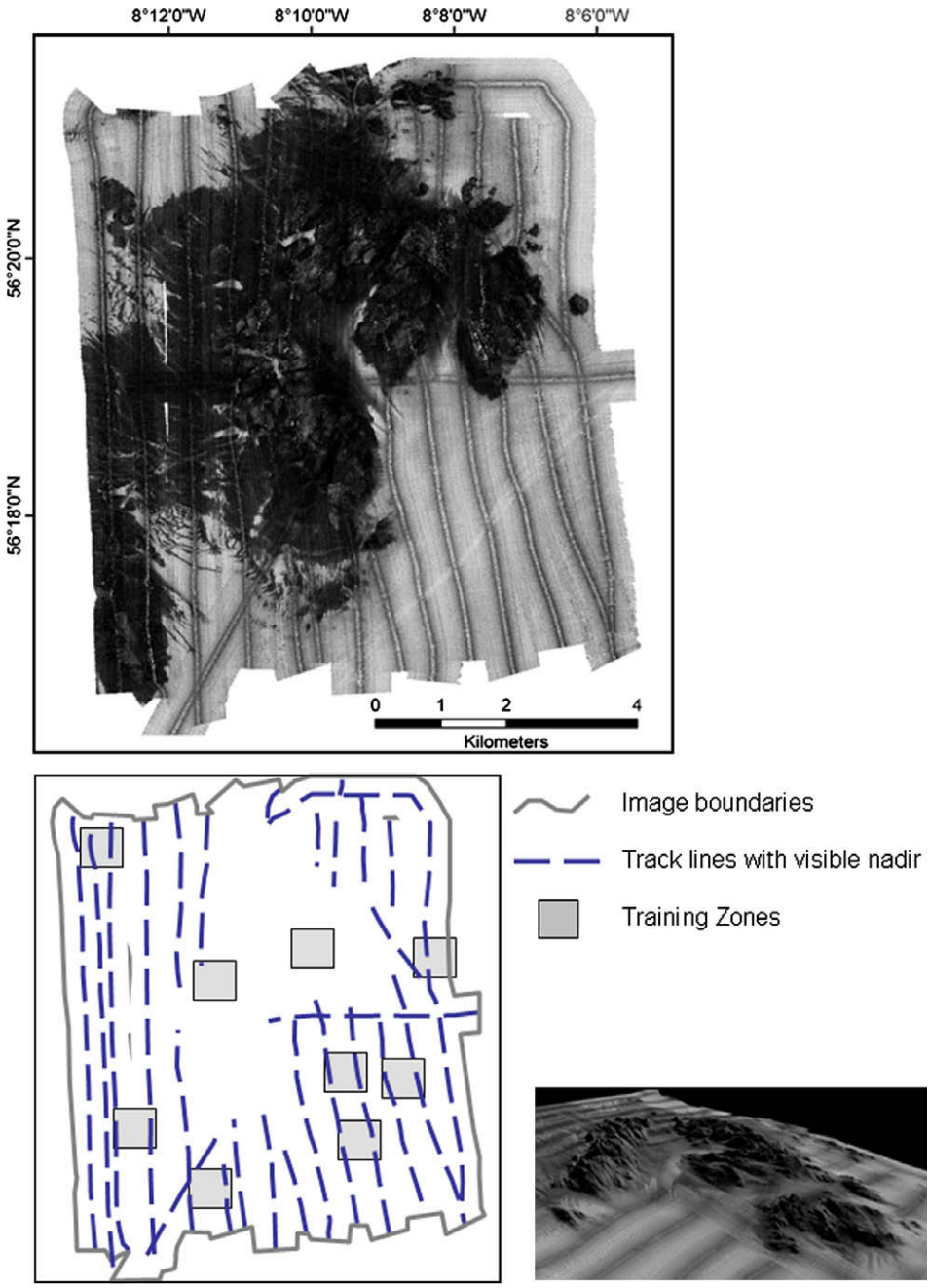

Fig. 2. Top: Multibeam imagery from Stanton Banks provided as part of the MESH dataset. High acoustic reflectivity is coded as dark. Bottom left: overlaid track lines with a visible nadir (note that a few lines cross at sub-perpendicular angles) The areas selected as Training Zones are shaded in grey. Bottom right: 3-D view of multibeam imagery draped on bathymetry.

Please cite this article in press as: Blondel Ph, Gómez Sichi O, Textural analyses of multibeam sonar imagery from Stanton Banks, ..., Appl Acoust (2008), doi:10.1016/j.apacoust.2008.07.015

for the distance (e.g. Mahalanobis and Euclidean) but our tests showed that a simple Euclidean metric was sufficient for this application. The use of other metrics would require a proper assessment of how physically appropriate they are for the type of data used. The K-Means algorithm is particularly suitable for clustering large amounts of data. It is made faster here by using initial values for the cluster centroids calculated using a random sample of 10% of the dataset. The total number of iterations necessary usually does not exceed 100 until convergence. The initial number of classes should be commensurate with the expected number of terrains to be classified. Adequate provision should be made for "mixed" classes, "unexpected" classes, etc. After K-means clustering, contextual editing can combine some of these classes if warranted by the application and supported by the ground-truth or other data. For sidescan imagery classification, the number of initial classes is generally close to the final number of distinct terrains. For multibeam imagery, the few examples so far ([19,20] and present study) seem to indicate that the number of initial classes should be substantially larger before reduction through contextual editing.

3. Application to multibeam imagery

3.1. Brief presentation of the dataset

The MESH dataset consists in multibeam bathymetry and imagery from the Stanton Banks and is presented in more details in Brown et al. (this issue). It was collected during a multibeam echosounder survey of the Stanton Banks by R/V Celtic Explorer in 2005, with a Kongsberg Simrad EM-1002 sounder, hull-mounted and operating at a frequency of 93–95 kHz [22]. The multibeam data were processed with the CARIS HIPS system, accounting for sound velocity variations, tides and basic quality control. The image is affected by a few artefacts, such as striping (noted in [22] but beyond immediate correction during processing). Imagery at the nadir has not been corrected either: regular lines with very high acoustic variability are visible along all tracks. The multibeam dataset was supplemented in summer 2006 with a ground-truthing cruise by R/V Corystes, which gathered a series of still photographs from the seabed in selected areas. The processed imagery was supplied as a GeoTIFF file, covering an area of approximately 8 by 9 km with a resolution close to 7 m/pixel (Fig. 2). This mosaic image, combining the different (already processed) survey lines, was used as input throughout this entire study. It shows a series of rock outcrops and plateaus (dark features in the centre of the image), generally less than 80 m higher than the surrounding sediments (light features in the image). The outcrops are incised by gullies and crevices, often filled in with sediments. The general background depths vary from 120 to 160 m. Ground truthing reveals that the SE sediments are made of mud, those in the SW of sandy mud and sand with pebbles closer to the outcrop.

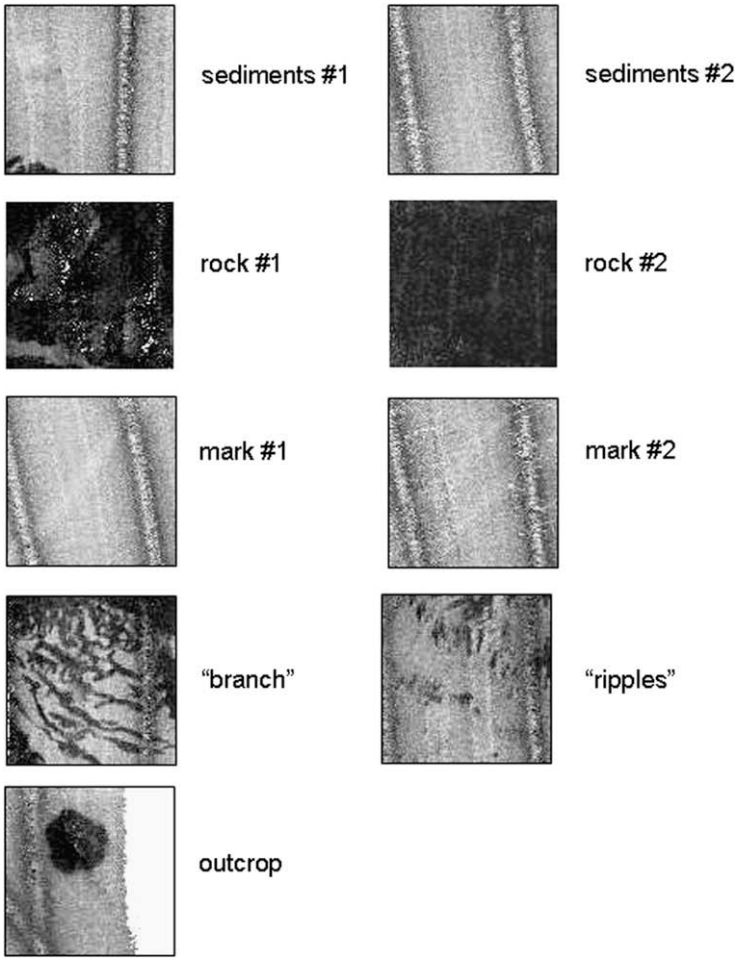

Fig. 3. Training Zones selected in representative portions of the imagery. Each image is 100 × 100 pixels wide, ensuring the number of derived entropy/homogeneity measurements remains statistically significant. These Training Zones are used to identify the optimal computation parameters for textural analyses with *TexAn*.

Please cite this article in press as: Blondel Ph, Gómez Sichi O, Textural analyses of multibeam sonar imagery from Stanton Banks, ..., Appl Acoust (2008), doi:10.1016/j.apacoust.2008.07.015

3.2. Training Zones

The selection of Training Zones in the mosaic image was performed before the ground-truthing exercise, and the different areas (highlighted in grey on Fig. 2) were chosen so as to cover representative sections of the entire multibeam image. Fig. 3 presents them in detail. Each Training Zone covers a square area of 100 × 100 pixels, ensuring the number of points for textural analyses varies from 8100 (for a window size of 10 pixels) to 1600 (for a window size of 60 pixels) and still remains statistically significant. Each zone is labelled with a generic description, sometimes just referring to its morphological appearance (e.g. "branch" or "ripples") to avoid premature interpreting. The Training Zone labelled "Sediments #1" was taken in the NW corner of the multibeam image, and corresponds to the shallow sediments. Another Training Zone, labelled "Sediments #2", was taken in the SE corner of the image, opposite, to look at the acoustic textures of the deeper sediments (later interpreted as mud during the ground-truthing exercise). Two Training Zones, respectively labelled "rock #1" and "rock #2", were taken in the outcrops in the centre of the image. The former corresponds to pinnacles (visible in the 3-D view draped over bathymetry: Fig. 2) and shows some degree of acoustic contrasts. The latter is poorly contrasted and shows a dark, mottled texture; it corresponds to the more rounded outcrops visible in the 3-D view of Fig. 2. Faint marks, tentatively interpreted as trawlmarks from their acoustic patterns and morphology, are visible in the image and two examples were taken as Training Zones (respectively labelled "mark #1" and "mark #2"). Although they occur in exactly the same sediments as the Training Zone "sediments #2", they were deemed interesting to investigate whether the perturbations induced by the trawlmarks could be detected from entropy and homogeneity variations. Another Training Zone ("branch") was taken in the area of ravines at the bottom of the outcrops, in the SW of the image. The southern end of the central outcrops is marked by a series of mottled acoustic patterns, presumably associated to changes in the sediments (sand/mud proportions), corresponding to the Training Zone labelled "ripples". Finally, the easternmost outcrop and its surrounding sediments were selected as a "combination" Training Zone, labelled "outcrop".

Systematic tests on the number of grey levels *NG*, the size *WS* of the computation window and the inter-pixel displacement *SZ* show an optimal separation for *NG* = 64, *WD* = 40, *SZ* = 25 (Fig. 4). The image is actually smoothed by using less grey levels than its full dynamic range and the speckle visible in some areas is filtered out from the textural calculations. Using more grey levels (e.g. 128 or 256) was shown to increase significantly the computation times, but not the quality of the overall classifications. The size of the computation window is commensurate with the scale of the structures visible on the image, and the inter-pixel displacement is close to *WS*/2, as seen in similar studies. With these parameters, there are 3600 individual measurements of entropy and homogeneity for each Training Zone. All sample areas can be clearly distinguished (Fig. 4). The zone labelled "rock #2" shows very low entropies and homogeneities; it was noted that the Training Zone was poorly contrasted (analysis reveals its grey levels are in fact mostly close to saturation). Sediments (in green) show large variations in homogeneity (i.e. the amount of local similarities) and smaller variations in entropy. They are clearly separated from the pinnacles (yellow) and

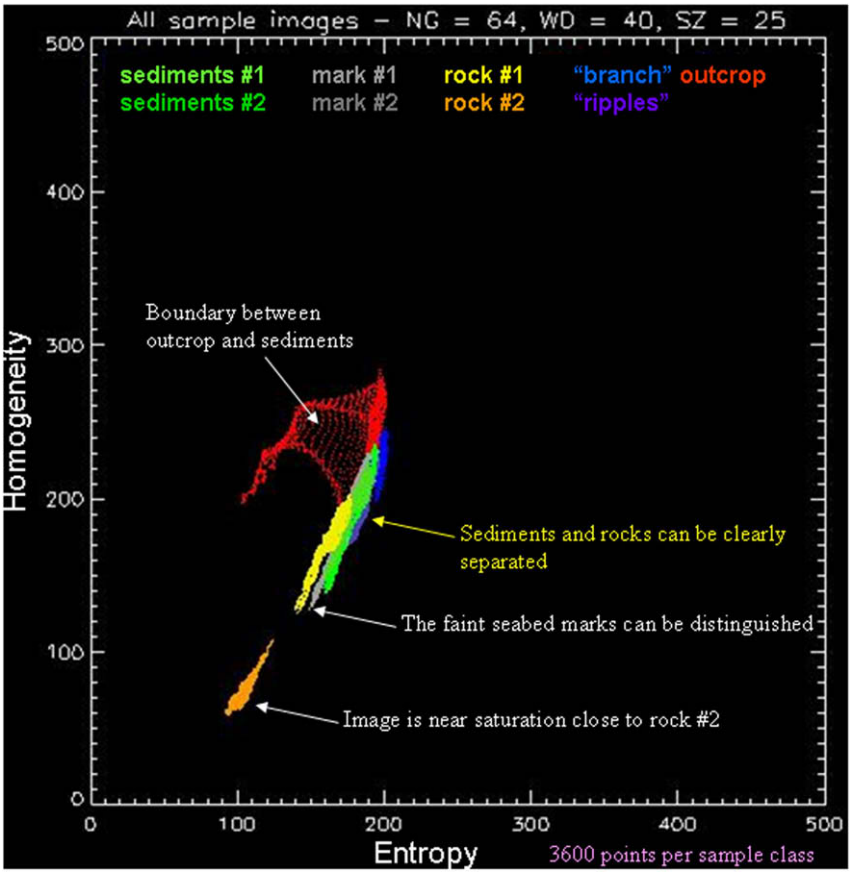

Fig. 4. Entropy-homogeneity values calculated for the Training Zones presented in Fig. 3. The optimal separation of the Training Zones in this feature space were obtained by systematically varying the number of grey levels *NG*, the size of the computation window *WS* and the inter-pixel displacement *SZ* (a full-colour version is available electronically). (For interpretation of the references in colour in this figure legend, the reader is referred to the web version of this article.)

Please cite this article in press as: Blondel Ph, Gómez Sichi O, Textural analyses of multibeam sonar imagery from Stanton Banks, ..., Appl Acoust (2008), doi:10.1016/j.apacoust.2008.07.015

outcrop (red). The faint trawlmarks on the seabed (in grey) can even be distinguished: their entropy/homogeneity values are smaller, but lie on the same trend. The "ripples" (light blue) (interpreted as varied sediments) are closely associated texturally to the other types of sediments, whereas the "branch" (blue) (associated to the sediment-filled ravines) are closer to the "outcrop" Training Zone (in red). The latter shows high variations in entropy and homogeneity, with characteristic "stripes" in the feature space corresponding to the boundary between the outcrop and the surrounding sediments. As the sliding computation window encompasses more of the outcrop, or more of the sediments, it will vary between the two textural end-members. More could be said at this level about the actual values (and extents) of entropy and homogeneity for each Training Zone, but the objective of optimising the computation parameters to distinguish the Training Zones has been achieved, and this can now be used on the entire image.

3.3. Texture-based classification

Entropy and homogeneity are now computed for every pixel in the mosaic image, using the optimal computation parameters identified in Section 3.2. K-means clustering is used in the manner

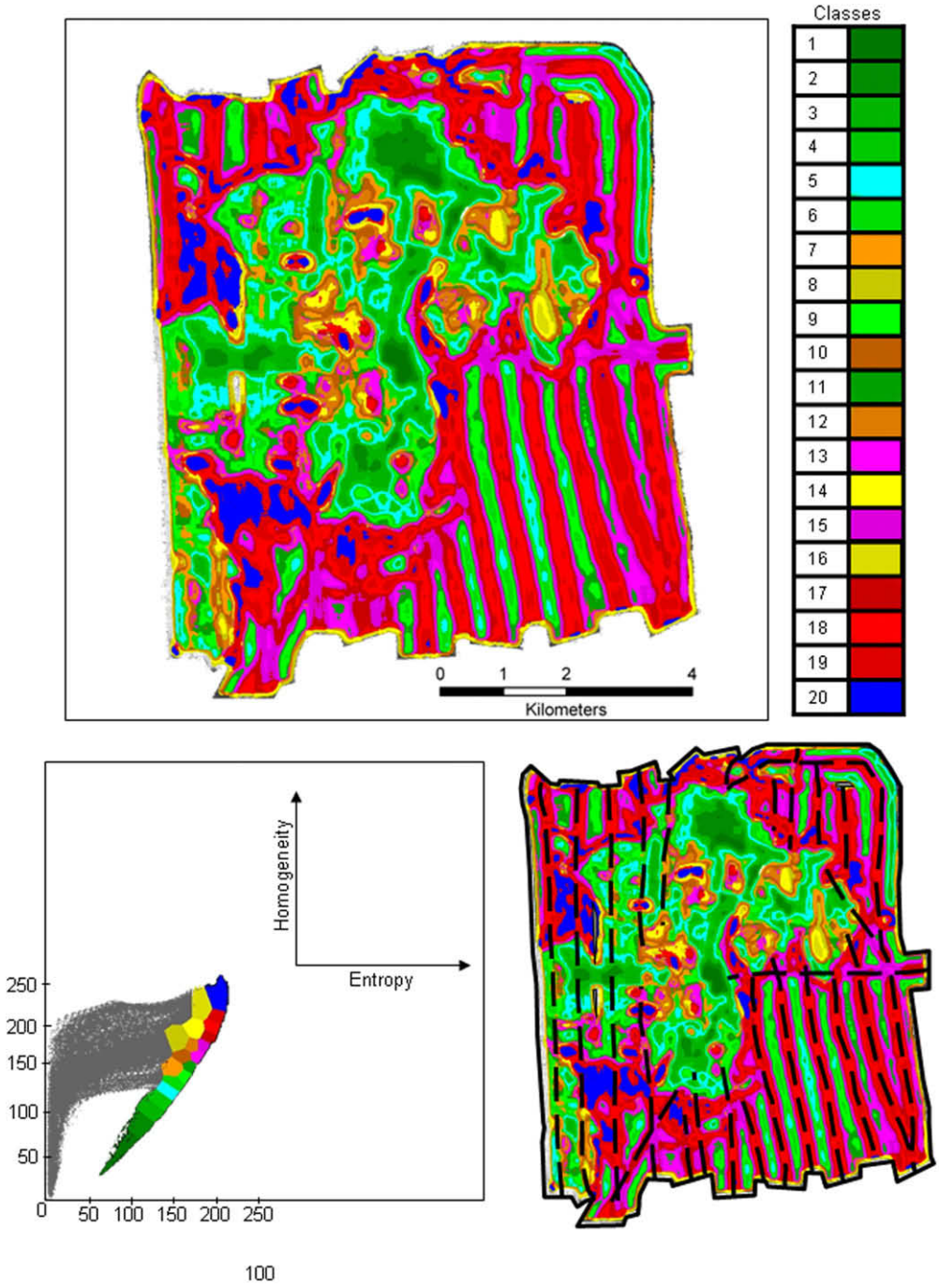

Fig. 5. *TexAn* classification (full-colour version available electronically). Top: fully classified image: each colour corresponds to one of the 20 textural classes identified through K-means and contextual editing (see text for details). Note that the colour scheme is different from that used for the Training Zones in Fig. 4. Bottom left: feature-space diagram showing the distribution of classes according to their entropy/homogeneity values. Points in grey correspond to the boundaries of the image. Bottom right: nadir lines and image boundary superimposed on the TexAn classification, showing the importance of full processing to refine the classification. (For interpretation of the references in colour in this figure legend, the reader is referred to the web version of this article.)

Please cite this article in press as: Blondel Ph, Gómez Sichi O, Textural analyses of multibeam sonar imagery from Stanton Banks, ..., Appl Acoust (2008), doi:10.1016/j.apacoust.2008.07.015

outlined in Section 2.3. Initial clustering in 14 classes [19] did not prove conclusive, as high levels of saturation in some areas and near-nadir artefacts induced abusive grouping of some terrains. Instead, 40 classes were initially created, in 98 iterations with a final convergence distance of 0.0. Some of them, corresponding to intermediate textures (i.e. boundaries and edges of image) were merged through contextual editing, and the final result of 20 classes is presented in Fig. 5. The entropy/homogeneity values of each cluster centre are clearly distinct, and they are presented in Table 1 with preliminary analyses of the different types of textures.

TexAn can clearly distinguish between the different terrains present in the image. The feature-space plot (Fig. 5, bottom left) shows the colour scheme adopted for each entropy/homogeneity cluster. The grey classes comprise only 6.4% of the image, despite their high entropy/homogeneity spread. They are associated to the edges of the multibeam image (as even pixels close to the edge were analysed), areas with no data (gaps in the mosaic) and a couple of very small, completely saturated areas. Classes coloured in dark green (lowest entropies, lowest homogeneities) correspond geographically to the outcrops, whose acoustic patterns show variable contrasts (as seen in the "rock #2"Training Zone). Lighter shades of green (slightly higher entropies and significantly higher homogeneities) correspond to sediments of increasing textural roughness, generally placed on the slopes of the outcrops and between the SE nadir lines. Increasing entropies and homogeneities (orange/brown/ochre tones) are associated to low-contrast boundaries between morphological regions. Classes coloured in purple to red tones relate to high-contrast boundaries and acoustically more contrasted sediments, either because of their roughness or because they are also affected by nadir artefacts. With lower entropies but similar homogeneities, yellow and dark yellow colours correspond to sediment infill within the ravines, and sediment ponding within the top of the different outcrops, generally in topographically rough terrain (hence with more variations in acoustic backscatter). With the highest entropies and homogeneities, a clearly distinct textural class, coloured in blue, is generally close texturally to the "branch" Training Zone. It is interpreted as ravines and gullies. The *TexAn* classification shows a few artefacts: for example, the wide nadirs are not classified properly (as expected). Better processing of the original image, by removing the influence of nadirs, should remedy to it. The faint trawlmarks visible in the image were distinguishable in the entropy/homogeneity feature space from the surrounding sediments (Training Zones "mark" vs. "sediments"). But these differences are very subtle, and in the course of K-means clustering, these regions are merged. A study interested in the trawlmarks themselves should start with a higher number of classes, or maybe even initialise one of the starting classes with the mean entropy/homogeneity values of these Training Zones.

4. Discussion

Overall, the *TexAn* classification works well, and the different types of terrains can be recognised fairly well from their acoustic textures. As it was made available after processing only, the localised ground-truth (see Fig. 2 of [8]) could not be used to define the Training Zones. It was, however, used to refine some of the interpretations and compared well with what can be deduced from acoustic textures. As interpretation of sonar imagery is increasingly carried out quantitatively with computers, the comparison with qualitative and visual interpretation is often used by non-specialists as a quick "measure" of how well a particular scheme works. However, the purpose of a real acoustic classification system should not be to emulate, in a visually pleasing manner, what a skilled interpreter could achieve, but to reveal additional patterns leading to a deeper analysis of the sonar imagery. Because it quantifies second-order statistics, *TexAn* does reveal differences in acoustic textures which can then be assigned to specific processes. Examples in this study included variations in sediments across the slopes of the outcrops (light green shades in Fig. 5). As hinted by ground-truthing, these subtle textural variations seem related to increasing local slopes and micro-scale roughness (e.g. rougher sediments, then small gravel, then pebbles/cobbles, and then talus).

Most uses of *TexAn* to date were with sidescan sonar imagery, and it is worth discussing the differences with multibeam sonar imagery and their potential impact on classification results. Sidescan instruments image a wide swath of seabed, with pixels across-track corresponding to slowly and continuously varying incidence angles [23]. These angles depend on the height of the sonar and its tilt; because sidescan sonars are usually flown close to the seabed, these incidence angles will be low and nearly grazing. Conversely, multibeam sonars are usually hull-mounted and hence higher above the seabed. Incidence angles will be high and vary by steps, because of beamforming at reception [24]. The way backscatter is derived (e.g. from mean energy or from snippets) will

Table 1
Entropy (E) and homogeneity (H) for the centres of the 20 data clusters resulting from K-means and contextual editing and presented as coloured classes in Fig. 5

E	H	Rough interpretation	Area (%)
92	62	Acoustically very homogeneous (generally close to saturation and/or with very poor contrasts), corresponding to the outcrops	0.4
113	84	Acoustically very homogeneous (close to saturation?) – mostly very flat areas	1.7
124	99	Sediments, including at base of slopes, slightly rougher textures	3.3
134	111	Sediments including at base of slopes	4.2
142	123	Acoustically reflective sediments on terrain becoming rougher (topographically)	5.7
148	133	"Wavy" sediments: slightly rough textures (including on topographically rough terrain)	7.1
150	148	Rough terrain (outcrops)	3.0
153	182	Sediments, including at the base of slopes in large gullies	1.4
157	141	Texturally homogeneous sediments: slightly rough textures (including on slopes)	6.7
159	162	Rough terrain (outcrops) (textures become rougher)	3.5
164	152	Sediments on fractured terrains, including on rough terrain	7.3
168	175	Rough terrain (outcrops) (rougher textures)	3.1
171	163	Acoustically reflective sediments (with nadirs included in the 0computation window + on slope boundaries)	7.2
172	193	Sediments at base of slopes in topographically rough terrain (talus? boulders?)	2.0
179	175	Texturally rougher sediments	8.3
179	218	Sediments at heads of crevaces/gullies	0.9
185	186	Acoustically contrasted sediments (nadir + on slope boundaries)	9.4
190	197	Acoustically contrasted sediments (nadir + on slope boundaries)	12.2
195	208	Acoustically contrasted sediments (nadirs + higher on slopes)	8.3
199	225	Ravined terrain (at all depths) (texturally and morphologically close to the "branches" Training Zone)	4.5

The rough interpretations are based on examination of the entire multibeam dataset and refined in the text using available ground-truth. The areas are percentages of the entire image area, rounded up to the first decimal.

Please cite this article in press as: Blondel Ph, Gómez Sichi O, Textural analyses of multibeam sonar imagery from Stanton Banks, ..., Appl Acoust (2008), doi:10.1016/j.apacoust.2008.07.015

also influence the local variations. These factors imply that computation windows will correspond to smaller angular variations in multibeam imagery, i.e. the textures will be more accurate representations of the seabed processes. But they also imply that the non-continuous variations in high incidence angles (potentially amplified by the processing) can yield artificial grey-level contrasts [25] and create more complex acoustic textures (i.e. additional variations in entropy and homogeneity).

One clear advantage of multibeam sonars over sidescan sonars is the constant co-registration of bathymetry and imagery, enabling the correction for true incidence angles [25] or at least the removal of the angular dependence of backscatter by referencing to a common angle [26–28]. This technique would also remove the high variations close to the nadirs, which greatly affect the present dataset (Fig. 2). Processing (and mosaicking) parameters have an important effect on resulting interpretation or quantitative analysis (e.g. [20,29]). Variations within individual swaths have been compounded here with the presence of tracks at acute angles to each other. Their mosaicking should account for the differences in imaging geometries, as it is not clear which part of the image was imaged from which direction: this could have been easily corrected when merging swaths referenced to a common angle. None of this reprocessing was performed here, as it was beyond the main objective of this study, namely the test of textural analyses on multibeam imagery. Although this affected the results of textural analyses, especially in flat, smooth sediments (Fig. 5), the main regions in the image could still be clearly delineated, and variations in some seemingly homogeneous regions (e.g. top of outcrops and sedimented slopes) could be revealed.

5. Conclusions

TexAn, a textural analysis technique, has been well validated on sidescan sonar imagery from a variety of contexts, including habitat mapping. Acoustic textures are quantified with Grey-Level Co-occurrence Matrices (GLCMs) and two indices, entropy and homogeneity (Section 2). These measurements can be merged into statistically meaningful groups with K-means clustering in particular. *TexAn* has been applied to a multibeam dataset acquired during the MESH project over Stanton Banks on the Irish continental shelf (Section 3). Optimisation of the processing parameters shows that a reduced number of grey levels (64, in this case) is sufficient, that the size of the computation window is commensurate with the scale of the structures visible on the image, and the inter-pixel displacement is close to WS/2, as seen in similar studies. Contextual editing is used to regroup obviously associated classes, yielding a final of 20 texturally different classes. Entropy and homogeneity variations are consistent with those expected from the Training Zones. *TexAn* can clearly distinguish between the different types of terrains and reveals in particular subtle variations in slope sediments. This is consistent with still photographs from the relevant portions of the seabed.

Because it was originally developed for a different type of sonar imagery, there are some limits to the use of *TexAn* with multibeam backscatter. The main one is the quality of the input data: unprocessed angular variations and the intersections of swaths at significant angles all limit the accuracy of the classification. But multibeam sonars provide some very positive points too. It was observed in Section 4 that subtle textural variations are related to increasing local slopes (i.e. the second derivative of the bathymetry) and to micro-scale roughness. This hints that classification might be improved by incorporating first-order statistics and depth-related information. Multi-dimensional clustering techniques exist to identify the optimal parameters (e.g. local contrast and slope variations) and they will need to be implemented cautiously, to ensure physically important variations in acoustic patterns are not lost in comparison with statistically more important background features. They will also need to be implemented transparently, to ensure that the physical meaning of these variations can still be assessed. First-order statistics can for example vary with the level of processing of the multibeam imagery, and this needs to be accounted for. This approach had shown promises in earlier work (Micallef and Blondel, unpublished, 2006) using sidescan imagery and multibeam bathymetry. The exact and accurate co-registration of imagery and bathymetry offered by multibeam sonars, along with the calibration of the backscatter measurements, make this approach more attractive for multibeam-only datasets.

This study is one of the first applications of *TexAn* analyses to multibeam backscatter. It does not pretend to be perfect, and more work needs to be done. Nonetheless, the results from unsupervised classification of entropy/homogeneity measurements using K-Means match well concurrent bathymetric data and later visual observations. Textural analyses successfully detect faint marks and distinguish the different types of seafloor, including variations within sediments, rocky outcrops and gullied terrains. The successful translation from sidescan to multibeam imagery is promising and opens new avenues for continental shelf mapping, and in particular habitat mapping.

Acknowledgements

The authors would like to thank Dr. Craig Brown for his original invitation to the data comparison workshop in 2006, and the officers, crews and scientists of R/V "Celtic Explorer" and R/V "Corystes" who made this exercise possible. The multibeam data presented here were collected as part of the Interreg IIIB Mapping European Seabed Habitats (MESH) project. This research was supported by the University of Bath. We thank Dr. Veerle Huvenne and an anonymous reviewer for their positive and constructive comments.

References

[1] Valentine PC, Cochrane GR, Scanlon KM. Mapping the seabed and habitats in National Marine Sanctuaries – examples from the east, gulf and west coasts. Mar Technol Soc J 2003;37(1):10–7.
[2] Kostylev VE, Todd BJ, Fader GBJ, Courtney RC, Cameron GDM, Pickrill RA. Benthic habitat mapping on the Scotian shelf based on multibeam bathymetry, surficial geology and seafloor photographs. Mar Ecol Prog Ser 2001;219:121–37.
[3] Christensen O. SUSHIMAP (Survey Strategy and Methodology for Marine Habitat Mapping). Norway: NTNU; 2006. <http://www.diva-portal.org/diva/getDocument?urn_nbn_no_ntnu_diva-1916-1__fulltext.pdf>.
[4] Anderson JT, Gregory RS, Collins WT. Acoustic classification of marine habitats in coastal Newfoundland. ICES J Mar Sci 2002;59(1):156–67.
[5] Brown CJ, Cooper KM, Meadows WJ, Limpenny DS, Rees HL. Small-scale mapping of sea-bed assemblages in the eastern English Channel using sidescan sonar and remote sampling techniques. Estuar Coast Shelf Sci 2002;54:263–78.
[6] Kenny AJ, Cato I, Desprez M, Fader G, Schuttenhelm RTE, Side J. An overview of seabed-mapping technologies in the context of marine habitat classification. ICES J Mar Sci 2003;60(2):411–8.
[7] Hühnerbach V, Blondel Ph, Huvenne V, Freiwald A. Habitat mapping on a deep-water coral reef off Norway, with a comparison of visual and computer-assisted sonar imagery interpretation. In: Todd B, Greene G, editors. Habitat mapping. Geological association of Canada special paper, vol. 47. p. 297–308, 2008.
[8] Brown CJ, Blondel Ph. A review of developments in the application of multibeam sonar backscatter data for seafloor habitat mapping. Appl Acoust, this volume.
[9] MESH, Development of a framework for Mapping European Seabed Habitats; 2007. <http://www.searchmesh.net/>.
[10] Blondel Ph. Segmentation of the Mid-Atlantic Ridge south of the Azores, based on acoustic classification of TOBI data. In: MacLeod CJ, Tyler P, Walker CL, editors. Tectonic, magmatic and biological segmentation of Mid-Ocean Ridges; 1996. Geological society special publication, vol. 118. p. 17–28.
[11] Blondel Ph. Automatic mine detection by textural analysis of COTS sidescan sonar imagery. Int J Remote Sens 2000;21(16):3115–28.
[12] Haralick RM, Shanmugam K, Dinstein I. Textural features for image classification. IEEE Trans Syst Man Cybern 1973;SMC-3:610–21.

[13] Reed TB, Hussong D. Digital image processing techniques for enhancement and classification of SeaMARC II side scan sonar imagery. J Geophys Res 1989;94(B6):7469–90.
[14] Blondel Ph, Sempéré JC, Robigou V. Textural analysis and structure-tracking for geological mapping: applications to sonar data from Endeavour segment, Juan de Fuca Ridge. Proc OCEANS'93, IEEE-OES 1993:209–13.
[15] Gao D, Hurst SD, Karson JA, Delaney JR, Spiess FN. Computer-aided interpretation of side-looking sonar images from the eastern intersection of the Mid-Atlantic Ridge with the Kane Transform. J Geophys Res 1998;103(B9):20997–1014.
[16] Cochrane GR, Lafferty KD. Use of acoustic classification of sidescan sonar data for mapping benthic habitat in the Northern Channel Islands, California. Cont Shelf Res 2002;22:683–90.
[17] Huvenne VAI, Blondel Ph, Henriet JP. Textural analyses of sidescan sonar imagery from two mound provinces in the Porcupine Seabight. Mar Geol 2002;188:323–41.
[18] Gómez Sichi O, Blondel Ph, Grácia E, Dañobeitia JJ. Quantitative textural analyses of TOBI sonar imagery along the Almería Canyon (Almería Margin, Alborán Sea, SE Spain). Geol Soc Special Pub 2005;244:141–54.
[19] Blondel Ph, Gómez Sichi O. TexAn seafloor characterisation – first tests with multibeam sonar imagery. In: MESH workshop proceedings; 2006.
[20] Huvenne VAI, Hühnerbach V, Blondel Ph, Gómez Sichi O, LeBas T. Detailed mapping of shallow-water environments using image texture analysis on sidescan sonar and multibeam backscatter imagery. In: Proceedings of the 2nd underwater acoustic measurements conference. Heraklion: FORTH; 2007 [on CD-ROM].
[21] Duda RO, Hart PF. Pattern classification and scene analysis. New York: Wiley; 1973.
[22] Cullen S, Wijntjes N, Hardy D. Irish National Seabed Survey – Leg CE 05_04, Zone 2. Geological survey of Ireland Cruise report; 2005.
[23] Blondel Ph, Murton BJ. Handbook of seafloor sonar imagery. Chichester: PRAXIS-Wiley; 1997.
[24] Lurton X. An introduction to underwater acoustics. Chichester: PRAXIS-Springer; 2002.
[25] Lurton X, Augustin JM, Dugelay S, Hellequin L, Voisset M. Shallow-water seafloor characterisation for high-frequency multibeam echosounder: image segmentation using angular backscatter. In: SACLANTCEN conference proceedings, vol. 45; 1997. p. 313–21.
[26] Preston JM, Christney AC. Compensation of sonar image data primarily for seabed classification. ECUA 2004:813–6.
[27] Augustin JM, Lurton X. Image amplitude calibration and processing for seafloor mapping sonars. IEEE Oceans 2005:698–701.
[28] Kloser R. Seabed backscatter, data collection and quality overview. In: Anderson JT, editor. Acoustic seabed classification of marine physical and biological landscapes, ICES cooperative research report, vol. 286; 2007. p. 45–60.
[29] Le Bas T, Huvenne V. Acquisition and processing of backscatter data for habitat mapping – comparison of multibeam and sidescan systems. Appl Acoust, this volume, doi:10.1016/j.apacoust-2008.07.010.

Please cite this article in press as: Blondel Ph, Gómez Sichi O, Textural analyses of multibeam sonar imagery from Stanton Banks, ..., Appl Acoust (2008), doi:10.1016/j.apacoust.2008.07.015